

10,04

Nonaffine deformations and local elastic properties of amorphous nanostructures

© A.A. Semenova, D.A. Konyuh, Ya.M. Beltyukov

Ioffe Institute
St. Petersburg, Russia
E-mail: aleksandr.semenov@mail.ioffe.ru

Received April 12, 2022

Revised April 12, 2022

Accepted April 14, 2022

Nonaffine deformations of amorphous nanostructures have been studied within the framework of a random matrix model. Near the boundary between amorphous and crystalline solids, nonaffine deformations of amorphous solids lead to the formation of a boundary region with altered effective elastic properties. It is shown that the thickness of the boundary region has the same order of magnitude as the scale of non-affine deformations. Keywords: nonaffine deformations, amorphous bodies, random matrices.

Keywords: nonaffine deformations, amorphous bodies, random matrices.

DOI: 10.21883/PSS.2022.08.54626.343

1. Introduction

In recent years, studies of mechanical, vibrational, and thermal conductivity properties of various nanostructured materials have become increasingly important. Among such materials, structures containing both crystalline and amorphous components are widely used. Misaligned arrangement of atoms inherent in amorphous bodies significantly affects both behavior of amorphous bodies on nanometer scale and their macroscopic properties. Macroscopic deformations of an amorphous body lead to heterogeneous local deformations, specific scale of which is estimated by tens of interatomic distances [1,2]. Such heterogeneous deformations are called *non-affine*, since they cannot be described by a combination of local extensions or shears. Non-affine deformations have been observed in many misaligned solids: metallic glasses [3], polymeric hydrogels [4], supercooled liquids [5], Lennard-Jones glasses [6], quartz glasses [7]. Non-affine deformations provide for important contribution to macroscopic elasticity properties.

For macroscopic description of elastic properties of amorphous bodies, classical elasticity theory using macroscopic moduli of elasticity can be applied. However, this method is not applicable to the description of microscopic deformations of nanostructures and nanocomposites containing amorphous regions, because in this case the characteristic scale of non-affine deformations R_{naff} may be comparable with typical dimensions of structural elements.

Recent research shows that in amorphous regions near their boundary with a stiffer body, a boundary region is formed, described by significantly higher elastic moduli compared to their values in the volume of the amorphous body. In paper [8], effect of nanoparticles on the local

elasticity of polystyrene around nanoparticles has been investigated using molecular dynamics method. Increase of elastic modulus of epoxy polymer near bimite nanoparticles was shown in paper [9].

In paper [8] it is shown that increase in local elastic modulus in the boundary region may not be due to a change in the local structure of the substance, but is caused by misaligned structure of the amorphous body itself. However, effect of misalignment on local elastic properties requires more detailed study.

In the present paper, in order to determine local elastic properties in the boundary region and their relation to non-affine deformations, we applied the random matrix model. Such a model has proven itself well in describing elastic and vibrational properties of amorphous solids, based on the most general assumptions about the properties of an amorphous body [10,11].

This article has the following structure. In Section 2, random matrix model used is formulated. In Section 3, specific scale of non-affine deformations as a function of misalignment degree in the system is determined. In Section 4, effect of boundary conditions on elastic properties of an amorphous body in the boundary region is shown. In Section 5, elastic properties of a nanostructure containing layers of amorphous and crystalline material are studied.

2. Random matrix model

The random matrix model [10] was applied to describe elastic properties of nanostructures with amorphous and crystalline phases. Such a model makes it possible to vary strength of misalignment and to describe both crystals and highly misaligned amorphous bodies. Besides, the random matrix model is based on the most general assumptions

about mechanical stability of an amorphous body and allows to describe universal vibrational and mechanical properties of amorphous bodies [10,11]. In this paper, the random matrix model will be applied to study elastic properties under quasistatic deformations.

For simplicity, this paper considers a simple cubic lattice with unit lattice constant $a_0 = 1$ and unit atomic masses $m_i = 1$. We use a scalar model, which assumes that the displacement of the i th atom, u_i , is a scalar quantity. Displacement u_i can be thought of as displacement along axis z in the direction of which external deformation will be applied.

To describe crystalline regions, the simplest model was considered, in which neighboring atoms are connected by single elastic bonds, and nonzero non-diagonal elements of the dynamic matrix have the form $M_{ij}^{(c)} = -1$ for neighboring atoms i and j . The rule of sums $M_{ii}^{(c)} = -\sum_{j \neq i} M_{ji}^{(c)}$ is satisfied for diagonal elements, which is related to invariance of the potential energy of the system with respect to displacing it as a whole. In the considered case of a simple cubic lattice $M_{ii}^{(c)} = 6$.

For amorphous regions, elements of the dynamic matrix are to some extent random variables. In this case, the requirement of mechanical stability plays an important role. In the most general form, a strongly misaligned stable mechanical system can be described by a dynamic matrix $M = AA^T$ [11]. Let us assume that matrix elements A_{ij} are Gaussian random numbers for neighboring atoms i and j . Just as in the construction of $M_{ii}^{(c)}$, the rule of sums $A_{ii} = -\sum_{j \neq i} A_{ji}$ is imposed on the matrix elements A .

To describe an amorphous phase with an arbitrary degree of misalignment, a dynamical matrix was considered in the form

$$M^{(a)} = AA^T + \mu M^{(c)}. \quad (1)$$

Dimensionless parameter μ controls the misalignment of the amorphous phase. $\mu \gg 1$ case describes a crystal with small fluctuations of the dynamic matrix elements. $\mu \ll 1$ case describes a strongly misaligned amorphous solid and is of most interest for the present paper.

3. Non-affine deformations

Because of local misalignment in the amorphous medium, which is described by the random matrix model (1), macroscopic deformation can cause local non-affine displacements.

Let us consider a sample $L \times L \times L$ in which the atoms have integer coordinates (x, y, z) and form a cubic lattice with a degree of misalignment μ . To study deformation of the amorphous medium, we apply single forces of opposite sign to each atom in the lower ($z = 0$) and upper ($z = L - 1$) layers. The sample has periodic boundary conditions along x and y directions, and open boundary conditions (Neumann boundary conditions) are used in z direction. Equilibrium displacements of atoms

u_i are determined by a system of linear algebraic equations

$$M^{(a)} u = F, \quad (2)$$

in which F — a column describing the force acting on the corresponding atom. Fig. 1, *a* shows resulting displacements for different degrees of misalignment μ . For each coordinate z , all displacements for atoms in a given layer are shown.

Displacements u_i can be decomposed into affine and non-affine components

$$u_i = u_i^{\text{aff}} + u_i^{\text{naff}}, \quad (3)$$

where the affine component is a linear function of z :

$$u_i^{\text{aff}} = az + b. \quad (4)$$

Distribution of the non-affine component u_i^{naff} is shown in Fig. 1, *b*. This distribution is Gaussian with zero mean and standard deviation σ_{naff} . To determine non-affine length scale, let us consider relative displacement between two atoms i and j caused by deformation

$$u_i - u_j = a(z_i - z_j) + (u_i^{\text{naff}} - u_j^{\text{naff}}). \quad (5)$$

For large distances $z_i - z_j$, relative displacement is determined by the first (affine) term of equation (5). However, for small distances $z_i - z_j$, relative displacement is determined by the random non-affine component. This allows us to estimate non-affine length scale as the distance at which affine and non-affine components have the same order of magnitude: $R_{\text{naff}} = \sigma_{\text{naff}}/a$. Fig. 1, *c* shows dependence R_{naff} on parameter μ . One can see that non-affine length scale has scale ratio

$$R_{\text{naff}} \propto \mu^{-1/4} \quad (6)$$

for $\mu \ll 1$. This ratio matches length scale of Ioffe–Regel l_{IR} , which represents a length of free passage of phonons near Ioffe–Regel frequency [10].

4. Influence of boundary conditions

Before turning to description of the amorphous nanosstructure, it is worth noting that the pattern of displacement distribution across the sample changes as the boundary conditions change. Instead of applying forces to the boundary atoms, we set their displacements at the boundary (Dirichlet boundary conditions). Let us assume that displacements of the atoms in the lower layer ($z = 0$) are zero $u_i = 0$, and in the upper layer ($z = L - 1$) single displacements $u_i = 1$ are given. In transverse directions (along x and y) the boundary conditions will still be periodic.

Fig. 2, *a* shows resulting equilibrium displacements of atoms u_i at a given displacement of the atoms at the upper and lower boundaries. Note that, in contrast to Fig. 1, *a*, spread of displacements at the edge of the sample decreases, which is caused by complete certainty of boundary displacements due to the boundary condition.

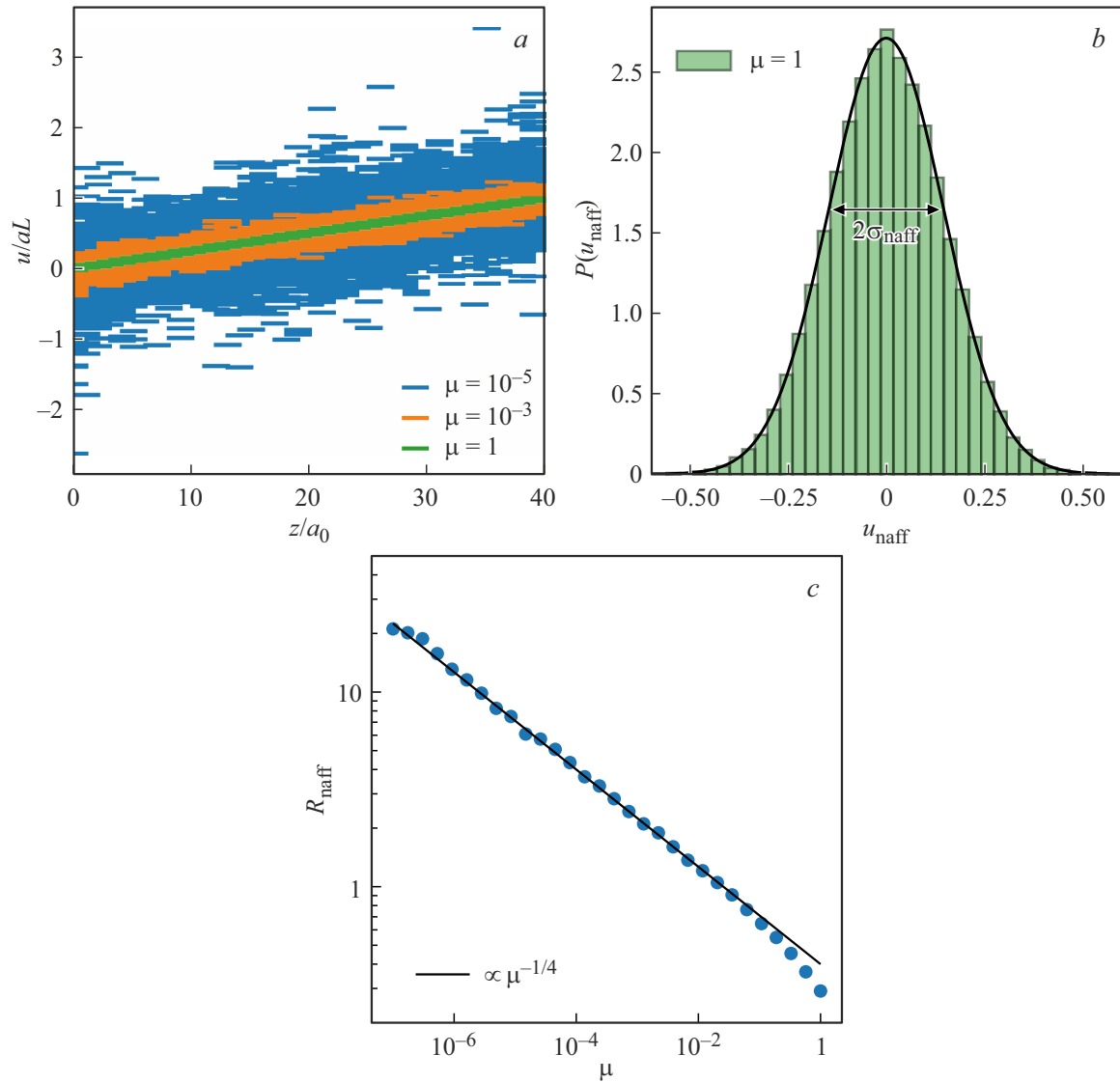


Figure 1. *a)* Displacements of atoms u_i as a function of coordinate z for an amorphous sample of size $L = 40$ at various values of parameter μ . Displacements are normalized so that the average displacement does not depend on the parameter μ . *b)* Distribution of the probabilities of non-affine displacement for case $\mu = 1$. Solid line — Gaussian distribution function with standard deviation σ_{naff} . *c)* Dependence of non-affine length scale on parameter μ .

Dependence of layer-averaged equilibrium displacements $\bar{u}(z)$ becomes markedly nonlinear — see Fig. 2, *b*.

Also note that in equilibrium the average mechanical stress σ is independent on coordinate z . Therefore, nonlinear dependence $\bar{u}(z)$ means uneven distribution of elastic properties along coordinate z . Besides, relationship between average mechanical stress σ and average deformation $d\bar{u}(z)/dz$ is determined by effective Young's modulus $E(z)$:

$$\sigma = E(z) \frac{d\bar{u}(z)}{dz}. \quad (7)$$

Corresponding effective ductility of the system is proportional to $d\bar{u}/dz$:

$$S(z) = \frac{1}{E(z)} = \frac{1}{\sigma} \frac{d\bar{u}(z)}{dz}. \quad (8)$$

In the scalar model under study, elastic modulus E and ductility S are scalar quantities [10]. The results obtained in this paper can be generalized to the case of a vector model, where corresponding quantities will be described by tensors of rank 4.

The resulting dependence of ductility $S(z)$ on coordinate z is shown in Fig. 2, *c* for different values of μ . It can be seen that ductility of the system near the boundary is lower than in the volume. At the same time, the size of the region with a reduced value of ductility depends on the degree of misalignment, which is controlled by parameter μ . Analysis of dependences $S(z)$ demonstrated their exponential behavior away from the boundaries. To determine specific size of the boundary region w , we approximated the dependence of $S(z)$ on the coordinate z

by the equation

$$S(z) = S_0 + S_1 \exp\left(-\frac{z-z_0}{w}\right) + S_1 \exp\left(-\frac{z_1-z}{w}\right), \quad (9)$$

where $z_0 = 0$ and $z_1 = L - 1$ — coordinates of upper and lower boundaries, accordingly.

Dependence of width of boundary region w on parameter μ is given on Fig. 3. It is seen that $w \sim \mu^{-1/4}$, which

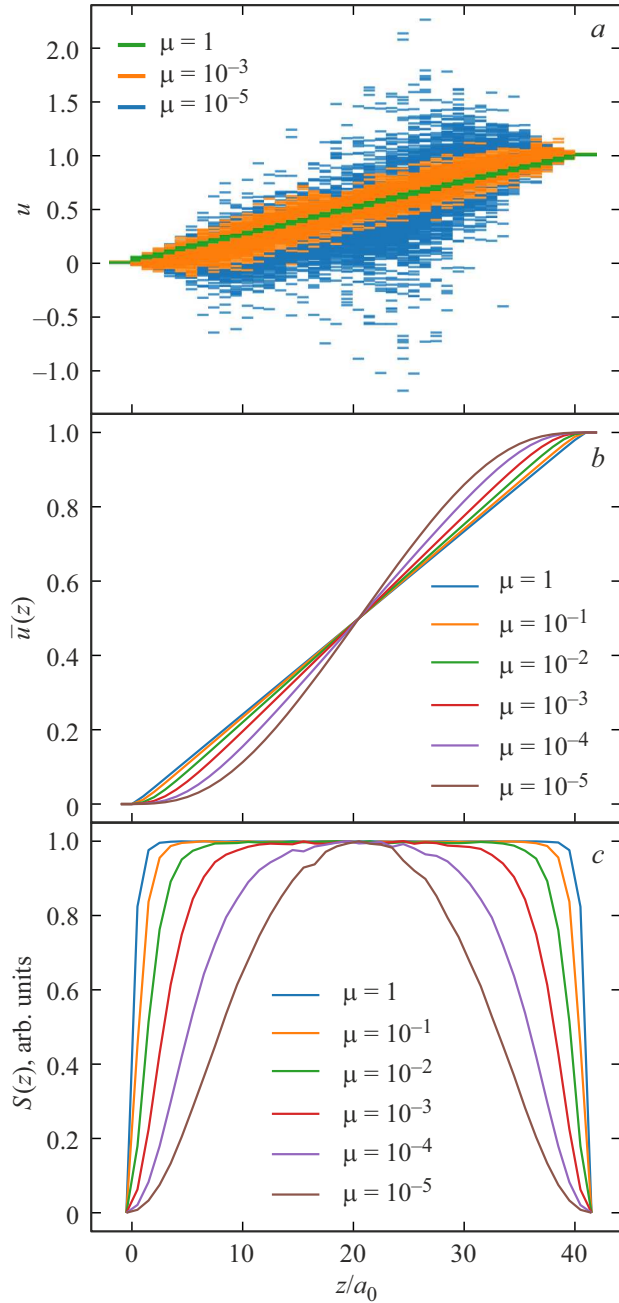


Figure 2. *a)* Equilibrium displacements of atoms u_i when setting displacements at the upper and lower boundaries of an amorphous body. *b)* Dependence of layer-averaged z equilibrium displacements for different values of parameter μ . *c)* Dependence of effective yield of $S(z)$ on coordinate z for different values of the parameter μ .

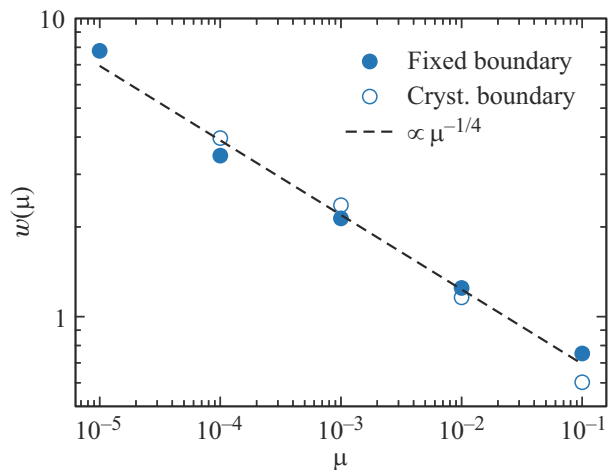


Figure 3. Dependence of boundary layer width w on value of parameter μ . Colored symbols comply with width of boundary layer for amorphous body with fixed boundaries. Open symbols comply with width of boundary layer for amorphous body in contact with crystalline line (see section 5). The line indicates dependence $w \sim \mu^{-1/4}$.

coincides with behavior of non-affinity radius R_{naff} , shown on Fig. 1, *c*.

The resulting heterogeneous ductility of the amorphous body (9) also affects elastic properties of the amorphous body as a whole. The average effective ductility of the amorphous body together with the boundary regions looks like

$$\bar{S} = \frac{1}{z_1 - z_0} \int_{z_0}^{z_1} S(z) dz \approx S_0 - 2 \frac{w}{L_a} S_1 \quad (10)$$

at $L_a \gg w$, where $L_a = L$ — full thickness of amorphous body. As a result, full ductility of amorphous body reduces by value proportionate to thickness of boundary region w .

5. Amorphous nanostructure

The results of the previous section demonstrated that amorphous body boundaries form effectively stiffer regions compared to regions in the volume of the medium if the boundary of the amorphous body is given as a non-deformable plane. In real structures, an amorphous medium may contact with a stiffer aligned medium, such as a crystal. In this case the crystal has finite stiffness, which may cause nonzero deformations of the crystal boundary due to non-affine deformations of the amorphous body.

For more detailed study of the interaction between non-affine deformations and effects at the crystal-amorphous body boundary, let us consider the three-layer $L \times L \times L$ nanostructure shown in Fig. 4, *a*. The central amorphous layer of thickness L_a is described by an amorphous dynamic matrix $M^{(a)}$ with given parameter μ . The external crystal layers are described by matrix $M^{(c)}$. The interfaces of the crystalline and amorphous phases have coordinates $z_0 = (L - L_a - 1)/2$ and $z_1 = (L + L_a - 1)/2$.

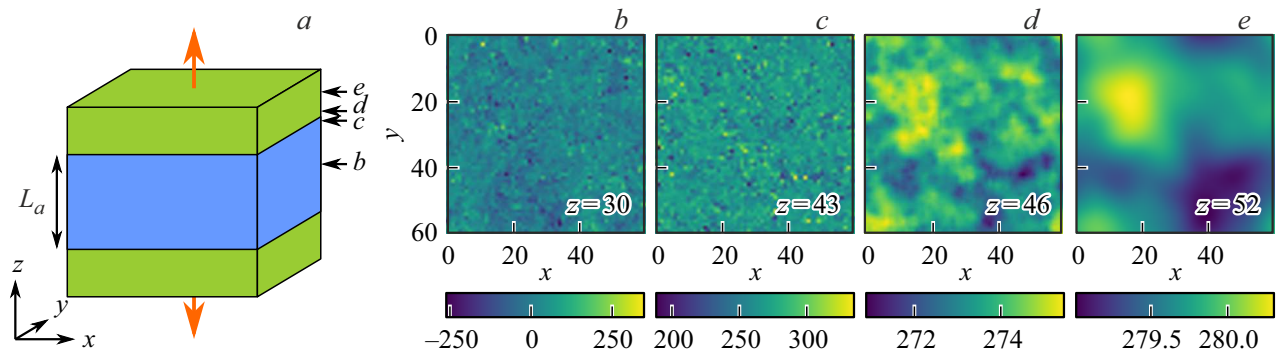


Figure 4. *a)* Layered nanostructure with a central amorphous layer (blue) and outer crystalline layers (green). Thickness of amorphous layer is $L_a = 30$. The total size of the nanostructure is $L \times L \times L$ at $L = 60$. All dimensions are counted in units of lattice constant a_0 . *b–e)* Equilibrium displacements u_i in different cross sections with given coordinates z , calculated for $\mu = 0.001$. These cross sections are indicated by arrows with corresponding letters on the panel (*a*).

For numerical simulations, we use system size $L = 60$ and $L_a = 30$, which is sufficient to study non-affine deformations (Fig. 4, *a*).

To study nanostructure deformation, we apply single forces of opposite signs to the lower ($z = 0$) and upper ($z = L - 1$) layers. For each realization of misalignment in the amorphous layer, we find equilibrium displacements u_i . Fig. 4, *b–e* shows equilibrium displacements u_i in different sections with given coordinates z in color. This figure demonstrates how non-affine deformations of an amorphous body propagate into the crystalline region.

To quantitatively analyze elastic properties of such a three-layer system, we considered equilibrium displacements u_i in various sections with given coordinates z , shown in Fig. 5, *a, b* and average displacement value $\bar{u}(z)$. Derivative $d\bar{u}(z)/dz$ allows us to determine ductility $S(z)$ according to equation (8). Resulting ductility $S(z)$ of the three-layer structure is shown in Fig. 5, *c* for different values μ . It can be seen that a boundary region with reduced ductility is formed near the crystal boundary.

To determine thickness of the boundary region, we will also use equation (9) to approximate ductility inside the amorphous layer. The resulting dependence of boundary region thickness w on parameter μ is shown in Fig. 3. Same as for fixed displacements of atoms at the boundary, dependence $w \sim \mu^{-1/4}$ is observed.

6. Discussion of results

Elastic properties of amorphous solids depend substantially on microscopic non-affine deformations. Using the random matrix model, it has been shown that radius of non-affine deformations depends on parameter μ as $R_{\text{naff}} \sim \mu^{-1/4}$. At such scales, the classical (continuum) theory of elasticity becomes inapplicable, since it is impossible to determine a smooth dependence of a displacement on the coordinate.

However, for structures whose statistical properties depend only on coordinate z , we can introduce a transverse

averaged displacement $\bar{u}(z)$ as a function of coordinate z . Behavior of such an averaged displacement is determined by effective Young's modulus $E(z)$ and corresponding effective ductility $S(z) = 1/E(z)$. In this case, dependence of ductility $S(z)$ on coordinate z depends substantially on the boundary conditions. For Neumann boundary conditions (when forces are applied to the boundary atoms), ductility $S(z)$ does not depend on coordinate z .

However, for Dirichlet boundary conditions (when displacement of the boundary atoms is set), ductility near the boundaries becomes significantly smaller than ductility away from the boundaries. This effect is due to the fact that any deformation of an amorphous body is accompanied by chaotic microscopic non-affine deformations, whose specific radius is determined by the size R_{naff} . Presence of a boundary with given displacements of atoms suppresses not only the average displacement of atoms, but also non-affine deformations. As a result, the medium becomes less ductile near the boundary, and specific size of such a region w is comparable to radius of non-affine deformations R_{naff} .

This effect is also observed for amorphous nanostructures, where an amorphous layer is located between two crystalline layers. In this case, non-affine deformations are not completely suppressed at the boundary, and some of non-affine deformations propagate into crystal depth. However, specific width of boundary layer w is also determined by radius of non-affine deformations R_{naff} .

The random matrix model is based on the most general assumptions about the properties of amorphous solids. This theory also allows us to describe such universal features of amorphous solids as boson peak and Ioffe–Regel crossover [10,11]. The random matrix theory demonstrates that frequency of boson peak coincides in order of magnitude with frequency of Ioffe–Regel crossover. Oscillations below Ioffe–Regel frequency have a certain wave vector and a certain free passage length, which exceeds the wavelength. At Ioffe–Regel frequency, free passage length becomes comparable to the wavelength, as a result, at higher frequencies it is impossible to describe

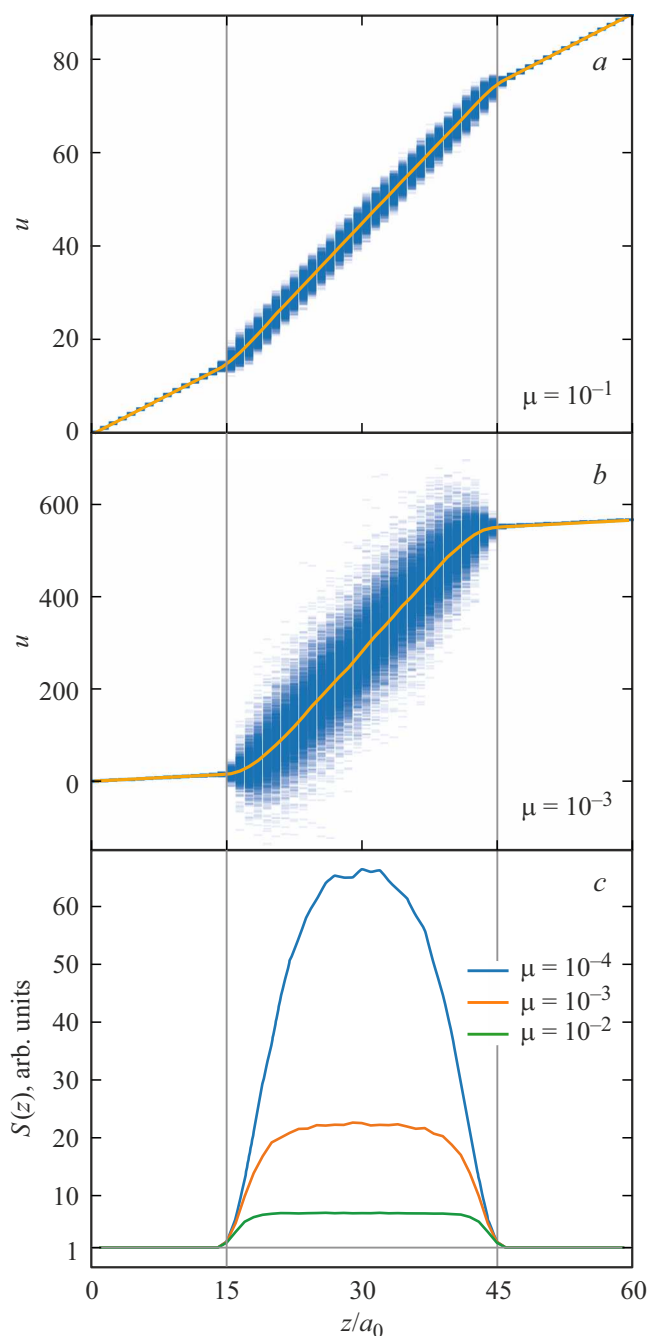


Figure 5. Displacements u_i in each of the layers z at $\mu = 0.1$ (a) and at $\mu = 0.001$ (b). The line shows averaging u_i over x and y . Vertical lines show interfaces z_0 and z_1 . c) Effective ductility for different values of μ .

oscillations by a certain wave vector, and propagation of such oscillations is of diffusive nature. Thus, at Ioffe–Regel frequency, free passage length acquires its minimal value l_{IR} among such range of frequencies, where the concept of free passage length is applicable to oscillations [10]. The results of this paper demonstrate that $R_{\text{naff}} \sim l_{\text{IR}} \sim \mu^{-1/4}$. Therefore, Ioffe–Regel length l_{IR} , the non-affinity radius R_{naff} and the thickness of the boundary region w have one

order of magnitude and separate the macroscopic scales to which classical (continuum) elasticity theory is applicable and the microscopic scales, where system misalignment plays an essential role.

The results of this paper are of great significance for physics of nanocomposites because they demonstrate that an effective stiffer shell can form around nanoparticles in a highly misaligned medium, size of which is determined by the non-affinity radius in such a misaligned medium, which depends on misalignment degree. For example, molecular dynamics calculations of polystyrene with SiO_2 nanoparticle show an increase in stiffness at the distance of about 1.4 nm around the nanoparticle [8]. For other amorphous substances, non-affinity radius was estimated to be about ten typical interatomic or intermolecular distances [2,7].

Direct experimental observation of elastic properties of a substance on scales of about of 1 nm can be difficult. However, results of this paper show a possible way to verify increase in stiffness of an amorphous body in the boundary region. A multilayered structure, where layers of amorphous material alternate with layers of a stiffer aligned body, will have a higher stiffness than a similar structure, where amorphous layers are combined into thicker layers. According to equation (10), the effect will be proportional to w/L_a , where L_a — thickness of a single amorphous layer.

7. Conclusion

This paper studied non-affine displacements in amorphous solids and amorphous-crystalline nanostructures. Using the random matrix model, a specific scale of non-affine deformations R_{naff} in amorphous solids was determined.

Effect of boundaries on elastic properties of an amorphous solid in the boundary region was determined. It was shown that both in fixed setting of amorphous body displacements at the boundary and in contact of an amorphous body with a crystalline one, a boundary region is formed with thickness w , where effective stiffness is higher than in the volume of an amorphous body. This phenomenon is due to the fact that, under such boundary conditions, non-affine deformations of an amorphous body at the boundary are suppressed, resulting in a decrease in effective ductility of a substance at distances of around the radius of non-affine deformations R_{naff} .

In this case, thickness of the boundary region w coincides in order of magnitude with non-affinity radius R_{naff} as well as Ioffe–Regel length l_{IR} , which plays a crucial role in vibrational properties of amorphous solids. The results obtained play an important role in understanding the macroscopic elastic properties of nanostructures and nanocomposites.

Funding

We would like to express gratitude for financial support to the Russian Science Foundation under grant No. 17-72-20201.

Conflict of interest

The authors declare that they have no conflict of interest.

References

- [1] C. Maloney. Phys. Rev. Lett. **97**, 035503 (2006).
- [2] F. Leonforte, R. Boissière, A. Tanguy, J. Wittmer, J.-L. Barrat. Phys. Rev. B **72**, 224206 (2005).
- [3] R. Jana L. Pastewka. J. Phys. Mat. **2**, 045006 (2019).
- [4] Q. Wen, A. Basu, P.A. Janmey, A.G. Yodh. Soft Matter **8**, 8039 (2012).
- [5] E. Del Gado, P. Ilg, M. Kroger, H.C. Öttinger. Phys. Rev. Lett. **101**, 095501 (2008).
- [6] C. Goldenberg, A. Tanguy, J.-L. Barrat. Eur. Lett. **80**, 16003 (2007).
- [7] F. Leonforte, A. Tanguy, J. Wittmer, J.-L. Barrat. Phys. Rev. Lett. **97**, 055501 (2006).
- [8] Y.M. Beltukov, D.A. Conyuh, I.A. Solov'yov. Phys. Rev. E **105**, L012501 (2022).
- [9] J. Fankhänel, B. Arash, R. Rolfs. Composites Part B **176**, 107211 (2019).
- [10] Y. Beltukov, V. Kozub, D. Parshin. Phys. Rev. B **87**, 134203 (2013).
- [11] D. Conyuh Y. Beltukov. Phys. Rev. B **103**, 104204 (2021).